BNL--46092

DE92 007599

EXAFS STUDIES OF BATTERY MATERIALS

James McBreen

Department of Applied Science
Brookhaven National Laboratory
Upton, NY 11973

X-ray absorption spectroscopy (XAS) has been used at extensively at Brookhaven National Laboratory (BNL) to study materials and electrodes of several battery systems. The power and the general applicability of the technique is illustrated by studies of several battery materials such as PEO-salt complexes, PbO_2, and **in situ** studies of mossy zinc deposition in alkaline electrolyte.

INTRODUCTION

The performance and life of batteries and fuel cells are often determined by the molecular aspects of materials structure and the kinetics of electrode processes. In the case of batteries long life requires the regeneration of chemicals in a reproducible form during each charging cycle. Fuel cells rely on active stable catalysts, so the molecular aspects of the processes are even more important. Identifying the key molecular processes in these devices has been difficult. The materials are often amorphous, and the electrodes and separators are usually composites with several components. The presence of the electrolyte precludes the use of methods that use electrons as a signal or probe. X-ray absorption spectroscopy (XAS) is an ideal method for **in situ** studies of battery and fuel cell materials because both the probe and signal are penetrating x-rays. The great advantage of the method is that the probe has a wavelength of atomic dimensions. Another advantage is that XAS is element specific, and this permits investigation of the environment of a constituent element in a composite material. The near edge part of the spectrum (XANES) provides information on oxidation state and site symmetry of the excited atom. The extended fine structure (EXAFS) gives structural information. Thus the technique provides both chemical and structural information. Since XAS probes only short range order it

can provide structural information on amorphous materials.

XAS WORK AT BNL

The general applicability of XAS to materials problems in batteries and fuel cells is illustrated by the variety of systems studied at Brookhaven in the past few years. This has included structure determinations of

1. Zn-Br complexes in Zn/Br_2 batteries
2. Zincate complexes in Zn/air batteries
3. RbBr-PEO (polyethylene oxide) complexes (25-120°C)
4. $ZnBr_2$-PEO complexes (25-120°C)
5. $Ni(OH)_2$ electrodes
6. Co additives in $Ni(OH)_2$ electrodes
7. Pt fuel cell catalysts in several acids
8. Poisons on Pt during methanol oxidation
9. UPD Cu, Pb and Sn on Pt catalysts
10. Pyrolyzed Co-TMPP and Fe-TMPP catalysts
11. Lead oxides including α-PbO_2 and β-PbO_2
13. Mossy zinc deposits in Zn/air batteries
14. Polymer organo-disulfide electrodes

Much of this work is covered in a series of recent publications (1-10). Several spectroelectrochemical cells have been developed for XAS in situ measurements in the transmission and fluorescence mode. This includes hermetically sealed cells for XAS studies on non-aqueous systems, at temperatures up to 150°C.

The present paper reviews XAS results on PEO-salt complexes and reports new results on XAS studies of formed PbO_2 plates, PbO_2 doped with Sb and in situ studies of mossy zinc in alkaline electrolytes. These diverse results illustrate the versatility of the XAS technique in studying battery systems.

XAS STUDIES OF PEO-$ZnBr_2$ ELECTROLYTES

Ion conducting polymers such as poly(ethylene oxide), PEO, $(CH_2-CH_2-O)_n$, contain a high density of donor heteroatoms and a sufficiently long hydrocarbon segment to allow cation solvation by a "cage" effect, where the donor electron doublets of the oxygen are directed inward. This solvation mechanism is reminiscent of that of the well known crown ethers. Unlike crown ethers, however, the cage size formed by the PEO chain can be adjusted to the size of the cation by taking advantage of the high degree of flexibility of the chain.

The solvation mechanism is both intra- and intermolecular and is reversible, a flexibility which allows the presence of ion pairs or multiplets and complex ions. This reversibility and conformational flexibility allows the ions to migrate from one solvating site to another, resulting in ionic conductivity.

The main problem with polymer electrolytes has been the low ion conductivity at room temperature, necessitating operation at elevated temperatures (80-100°C). At temperatures below ≈60°C, the tendency of PEO-salt complexes to form crystalline complexes leads to a drastic reduction in ion conductivity due to an almost complete disappearance of the conducting elastomeric phases. The room temperature conductivities are in the 10^{-7} - 10^{-8} S/cm range or lower. Conductivities in the 10^{-4} - 10^{-5} S/cm range are generally required for efficient operation of thin film electrochemical devices.

One approach to improve conductivity of polyethylene oxide (PEO)-salt systems is to modify the polymer to increase the mobility of the ions. Modifications involve the addition of plasticizers or the synthesis of polymer structures to promote facile segmental chain motion in the polymer. These approaches are based on the idea that ion mobility is controlled by the dynamics of the polymer host. Conductivity also depends on ion pairing, Coulombic interactions among ionic carriers and interactions of the ions with the host polymer. So far we have very little information on these aspects. It is difficult to obtain this type of information for PEO-lithium salt electrolytes. However, this type of information can be obtained from EXAFS for PEO-salt complexes of heavier metals. Recently both (PEO)-$ZnBr_2$ and (PEO)-RbBr complexes were investigated in the temperature range 25°C to 120°C (2). In both complexes the results at all temperatures were similar and were consistent with the

presence of largely undissociated $ZnBr_2$ or RbBr species. In the case of (PEO)-$ZnBr_2$ complex, the $ZnBr_2$ species were coordinated with four oxygens from the PEO. A model based on the results is shown in Figure 1. The respective calculated Zn-Br and Zn-O bond lengths were 2.34 Å and 2.23 Å. There is evidence of some $ZnBr_2$ dissociation at higher temperatures. A mechanism, based on Br^- ion hopping between anchored species of $ZnBr_2$ and $ZnBr^+$ in PEO, is proposed to explain reported transport number and conductivity data. The results show that if high conductivity is to be achieved attention has to be paid factors influencing both ion dissociation and ion mobility.

XAS STUDIES OF THE PbO_2 ELECTRODE

Recently an extensive XAS study was made of several lead oxides and salts (10). The oxides included PbO_2 prepared by the various methods described by Bagshaw et al. (11). Figure 2 shows normalized XANES spectra for Pb, yellow PbO, Pb_3O_4 and β-PbO_2 deposited from perchlorate solutions. The XANES for the oxides have various shoulders and distortions which decrease the edge shifts. Nevertheless, there is an orderly increase in the edge energy in going from PbO to Pb_3O_4 to β-PbO_2. The shoulders and distortions in the XANES features for the oxides can be explained on the basis of hybridization, site symmetry and crystal field splitting effects. In the case of PbO_2 there is a well defined pre-edge peak, at -5 eV, due to electronic transitions from the 2p into the empty 6s states. A comparison of the pre-edge peak for PbO_2 samples, prepared by various methods, shows that there is a good correlation between the intensity of this peak and the stoichiometry of the PbO_2. This is illustrated in Figure 3. The electrochemical deposited material is essentially stoichiometric PbO_2, whereas the material prepared by acetate hydrolysis has a lower stoichiometry ($PbO_{1.86}(OH)_{0.20}$) and α-PbO_2 has the stoichiometry $PbO_{1.83}(OH)_{0.14}$ (11). The peak intensity decreases with reduced oxygen stoichiometry. Results in Figure 4 show that the addition of Sb to the perchlorate electrolyte reduces the intensity of the pre-edge peak. A comparison of the XANES for PbO_2 electrodeposited from perchlorate electrolyte and PbO_2 in a formed battery plate is shown in Figure 5. Again there is a reduction in the intensity of the pre-edge peak. The increased electrochemical activity of formed battery plates as compared to chemically prepared or electrodeposited β-PbO_2 must be related to the lower oxygen stoichiometry. Also the beneficial effect of Sb must be also related to a reduction in oxygen stoichiometry.

XAS STUDIES OF MOSSY Zn DEPOSITS

Zinc deposition from alkaline zincate electrolytes is unusual in that finely divided mossy deposits are formed at low current densities (12). In the case of other metals finely divided deposits are only formed at very high current densities (13). Recently an **in situ** XAS study of zinc deposition in alkaline electrolyte was started at BNL.

Experimental

The zinc deposition studies were carried out in the cell shown in Figure 6. XAS spectra were recorded for the zincate electrolyte, prior to zinc deposition. Zinc was deposited under potentiostatic conditions (-45 mV or -65 mV vs. a Zn wire reference) in a thin cavity (~0.5 mm). After sufficient zinc was deposited to fill the cavity above the level of the x-ray window, transmission XAS measurements were made, with the electrode still under potential control. XANES measurements were also recorded, on the zinc deposited at -65 mV, over a one hour period after switching the electrode to open circuit. A XAS spectrum was also obtained for zinc foil.

Results and Discussion

Figure 7 shows a comparison of the radial structure functions (RDF) for zinc foil, the zincate solution and mossy zinc deposited at -45 mV and -65 mV. The first peak in the RDF for the zincate solution corresponds to the Zn-O coordination in the zincate ion. The first peak in the RDF for zinc foil is the Zn-Zn contribution of the nearest 12 Zn atoms. Because of the distortion of the hexagonal structure this peak is actually the contribution of two coordination shells, one with 6 atoms at 2.670 Å and the other with 6 atoms at 2.892 Å. In the case of the zinc deposit at -65 mV there is no Zn-O contribution in the RDF. This indicates that at this potential the electrolyte in the electrode pores is exhausted of zincate and contains only pure KOH electrolyte. However, at -45 mV, there is a Zn-O contribution, indicating the presence of zincate in the electrode pores.

Figure 8 shows an expanded view of the first Zn-Zn peak in the RDF for zinc foil and for mossy zinc deposited at -45 mV and -65 mV. The peak maximum for the mossy zinc at -65 mV is shifted to a lower **r** value. The x-rays from a synchrotron are highly polarized with the polarization vector oriented in the plane of the ring. Work on zinc single crystals has shown that the peak in the **r** value

depends on whether the **a** axis or **c** axis is oriented parallel to the polarization vector (14). The present results indicate that the deposit at -65 mV is oriented with the **c** axis parallel to the lines of current. The polarization vector is parallel to the **a** axis and only the smaller 2.670 Å shell contributes to the spectrum. The deposit at -45 mV must have a random orientation like that in the zinc foil.

XANES Results

Figure 9 shows a comparison of normalized XANES spectra for Zn foil, a zincate solution and the zinc deposit at -65 mV and -45 mV. The white line peak at 10 eV is higher for the zincate solution. The presence of zincate in the deposit at -45 mV also increases the intensity of the white line. There are some modifications in the XANES for the deposit at -65 mV, when compared to zinc foil. This may be an orientation effect.

Figure 10 shows a comparison of the XANES spectra, for the deposit at -65 mV, that were taken at various intervals after switching to open circuit. The results are consistent with an increase of zincate within the pores of the deposit. As long as there is a deposition at -65 mV, the concentration of zincate within the deposit is essentially zero. However, on going to open circuit the zincate concentration within the deposit builds up. This buildup can occur either by diffusion of zincate into the electrode pores or by the generation of zincate within the pores by concentration cell effects. The latter are possible because, on switching to open circuit, the electrolyte in the pores is essentially pure KOH, whereas the electrolyte at the mouth of the pores, on top of the deposit, is a concentrated zincate solution. The resultant concentration cell, would dissolve zinc in the interior of the pores and deposit zinc at the mouth of the pores . The speed with which the concentration of zincate in the pores builds up strongly suggests a concentration cell effect.

ACKNOWLEDGMENT

The author gratefully acknowledges support of the U.S. Department of Energy, Division of Materials Sciences, under Contract Number DE-FG05-89ER45384 for its role in development and operation of Beam Line X-11 at the National Synchrotron Light Source (NSLS). The NSLS is supported by the Department of Energy, Division of Materials Sciences under Contract Number DE-AC02-76CH00016. The formed

battery plates were provided by Dr. K. Bullock of Johnson Controls.

REFERENCES

1. J. McBreen and I.-C. Lin, J. Electrochem. Soc., accepted for publication, (BNL-46091), 1991.

2. T. A. Skotheim, X. Q. Yang, K. H. Xue, H. S. Lee, J. McBreen and F. Lu, Electrochim. Acta, submitted for publication, (BNL-46453), 1991.

3. D. Guay, G. Tourillon, E. Dartyge, A. Fontaine, J. McBreen, K. I. Pandya and W. E. O'Grady, J. Electroanal. Chem., 305,83(1991).

4. J. McBreen, W. E. O'Grady, G. Tourillon, E. Dartyge and A. Fontaine, J. Electroanal. Chem., 307, 229(1991).

5. K. I. Pandya, W. E. O'Grady, D. A. Corrigan, J. McBreen and R. W. Hoffman, J. Phys. Chem., 94, 21(1990).

6. K. I. Pandya, R. W. Hoffman, J. McBreen and W. E. O'Grady, J. Electrochem. Soc., 137, 383(1990).

7. J. McBreen, Proc. Symp. on Nickel Hydroxide Electrodes, D. A. Corrigan and A. H. Zimmerman, eds., The Electrochemical Society Pennington, NJ (1990), pp. 61-81.

8. J. McBreen, W. E. O'Grady, G. Tourillon, E. Dartyge, A. Fontaine and K. I. Pandya, J. Phys. Chem., 93, 6308(1989).

9. J. McBreen, W. E. O'Grady, K. I. Pandya, R. W. Hoffman and D. E. Sayers, Langmuir, 3, 428(1987).

10. J. McBreen, Extended Abstracts, 179th Meeting of The Electrochem. Soc., Abstract No. 799, The Electrochem. Soc., Pennington, 1991.

11. N. E. Bagshaw, R.L. Clarke and B. Halliwell, J. Appl. Chem., 16, 180(1966).

DISCLAIMER

12. J. McBreen and E. J. Cairns, Advances in Electrochemistry & Electrochemical Engineering, Vol. 11, H. Gerischer and C. W. Tobias, eds., Wiley, New York (1978) p.273.

13. N. Ibl, Advances in Electrochemistry & Electrochemical Engineering, Vol. 2, P. Delahay and C. W. Tobias, eds., Wiley, New York (1962) p. 49.

14 G. S. Brown, P. Eisenberger and P. Schmidt, Solid State Comm., 24, 201(1977).

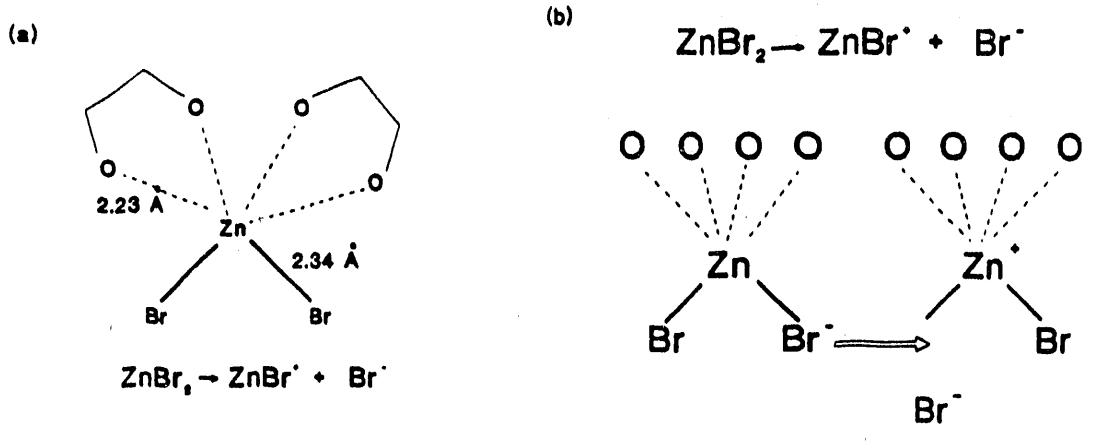

Figure 1. (a) Chemical structure of PEO-$ZnBr_2$ as determined by EXAFS. (b) Model for Br^- hopping mechanism to explain high conductivity and low Zn transport number.

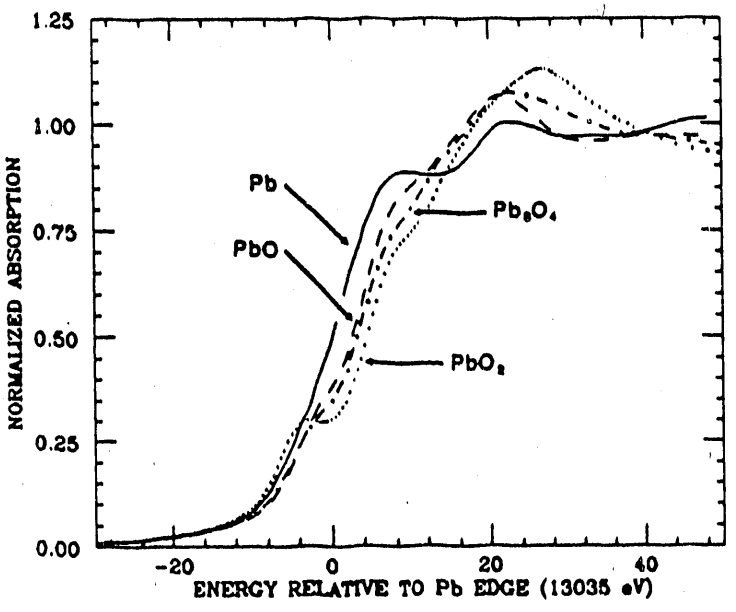

Figure 2. Normalized XANES spectra for Pb, PbO, Pb_3O_4 and PbO_2.

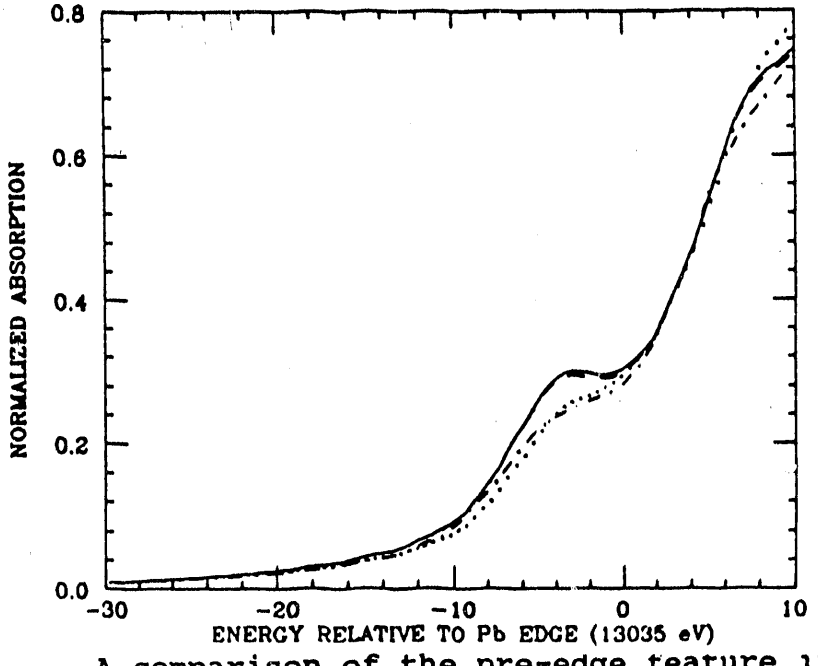

Figure 3. A comparison of the pre-edge feature in PbO_2 XANES for PbO_2, with different stoichiometries, when prepared by various methods; (a) electrodeposition from perchlorate (---), (b) minium oxidation(- - -), (c) acetate hydrolysis (-·-·-) and (d) oxidation in a perchlorate melt (····).

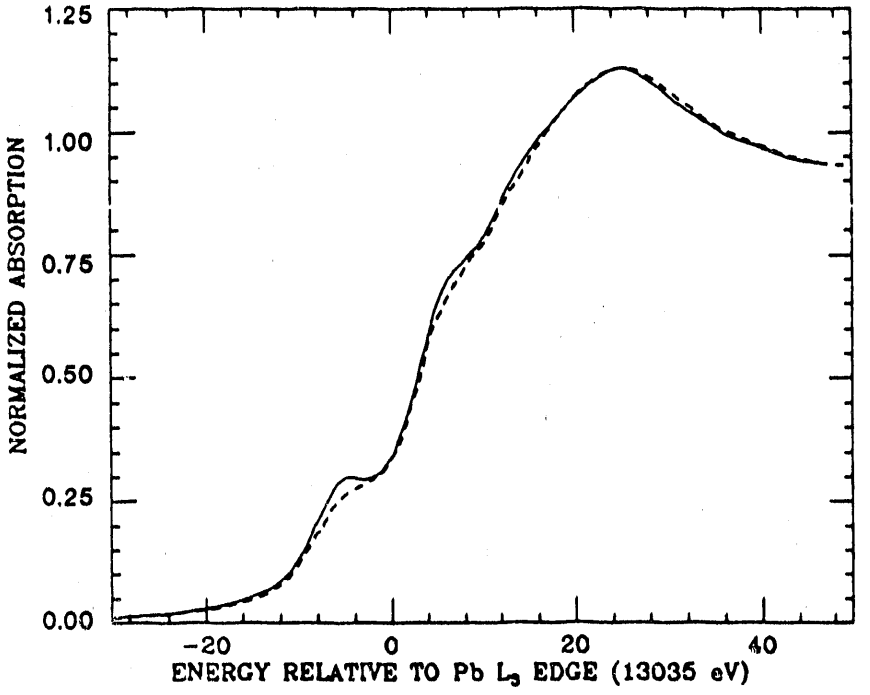

Figure 4. A comparison of the normalized XANES for PbO_2 deposited in pure perchlorate (——) and in perchlorate containing 10^{-5} M Sb^{3+} (---).

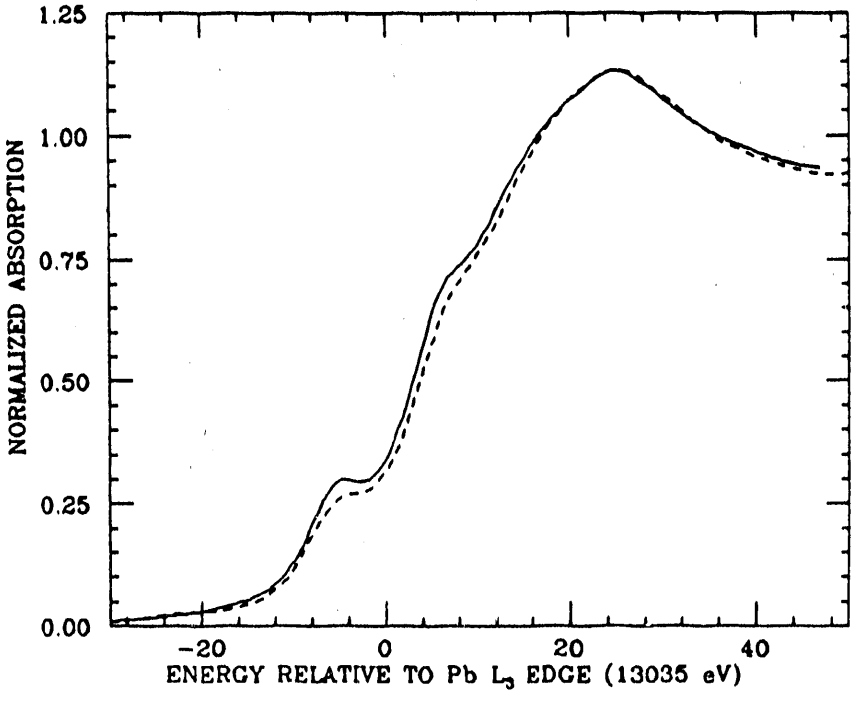

Figure 5. A comparison of the normalized XANES for PbO_2 deposited in perchlorate (——) and PbO_2 from a formed battery plate (---).

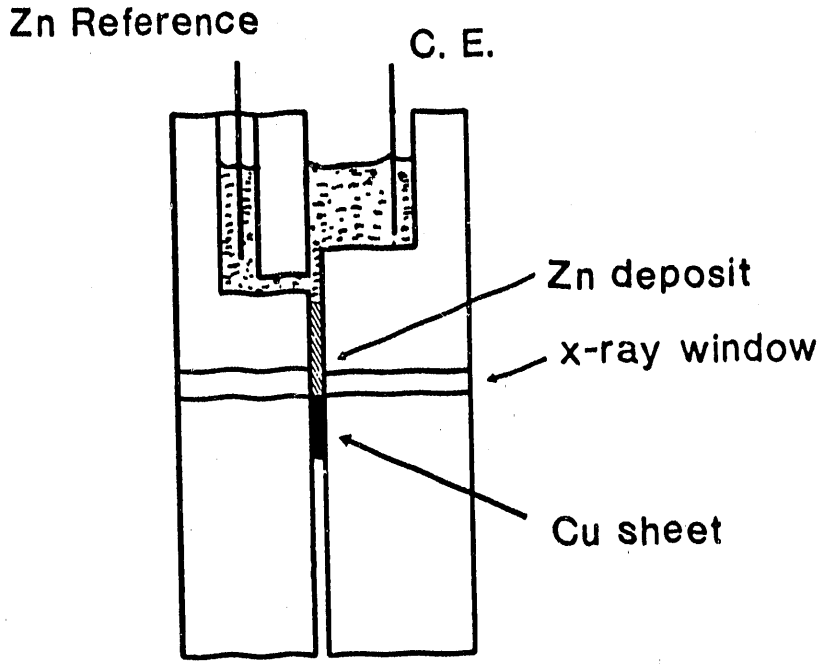

Figure 6. Cell for **in situ** XAS studies of Zn deposits.

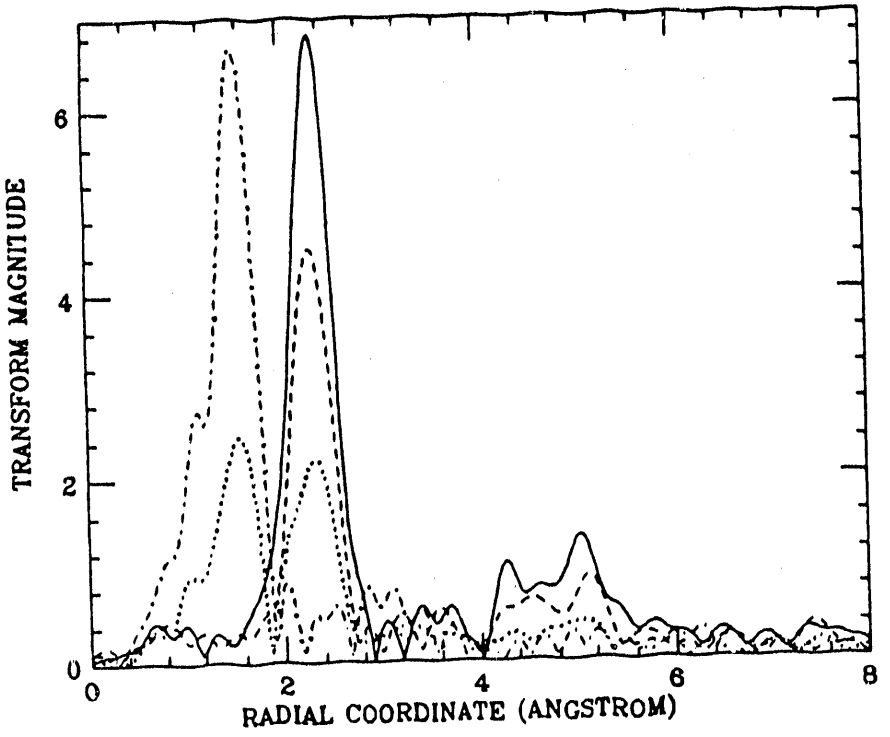

Figure 7. A comparison of RDFs for Zn foil (——), zincate solution (-•-•-), Zn deposited at -65 mV (----) and Zn deposited at -45 mV (••••), (Δk = 2.7 - 15.2 $Å^{-1}$).

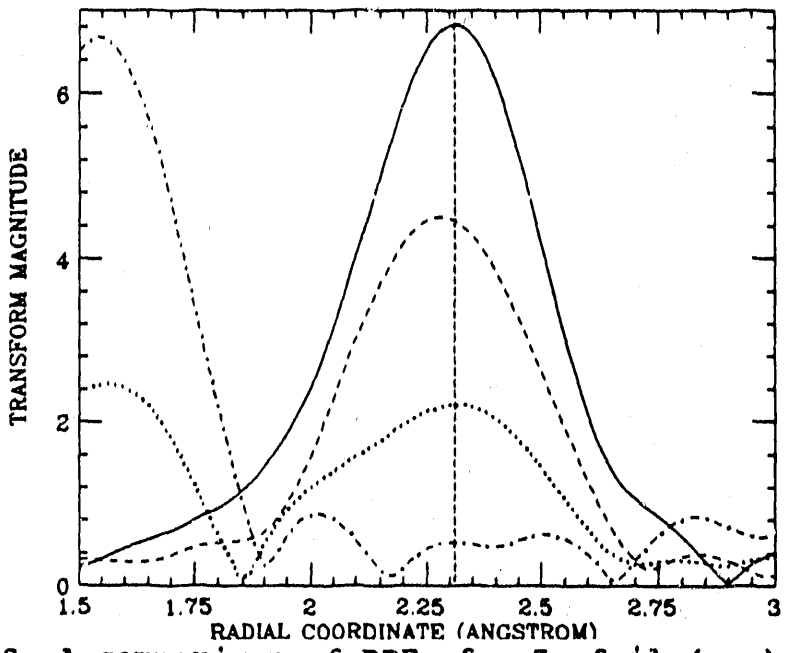

Figure 8. A comparison of RDFs for Zn foil (——), zincate solution (-•-•-), Zn deposited at -65 mV (----) and Zn deposited at -45 mV (••••), over the range Δr = 1.5 - 3.0 Å.

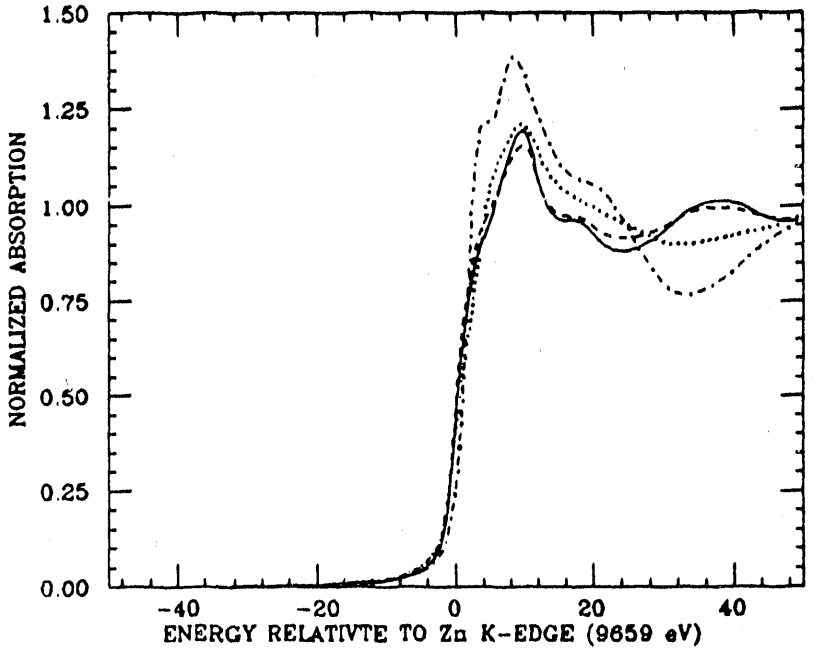

Figure 9. A comparison of normalized XANES for Zn foil (——), zincate solution (-•-•-), Zn deposited at -65 mV (----) and Zn deposited at -45 mV (••••).

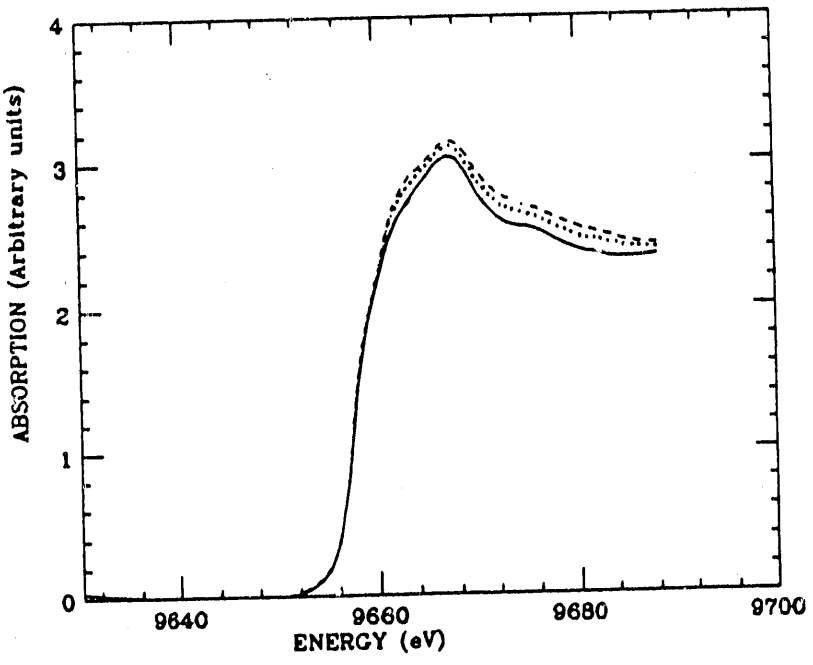

Figure 10. A comparison of the XANES spectra for the deposit at -65 mV, after various times on open circuit, 23 min. (——), 48 min. (••••) and 63 min. (----).

END

DATE FILMED

3/11/92